LNF-811036--1

LA-UR -81-2622

Los Alamos National Laboratory is operated by the University of California for the United States Department of Energy under contract W-7405-ENG-36

TITLE MICROSEISMIC ACTIVITY OBSERVED DURING DEPRESSURIZATION OF AN OIL STORAGE CAVERN IN ROCK SALT

AUTHOR(S) James Albright, G-7, Christopher Pearson, G-7

SUBMITTED TO Third Conference on Acoustic Emission/Microseismic Activity in Geologic structures and Materials, October 5-7, 1981, University Park, PA, to be included in the proceedings.

Los Alamos Los Alamos National Laboratory

MICROSEISMIC ACTIVITY OBSERVED DURING DEPRESSURIZATION OF AN OIL STORAGE CAVERN IN ROCK SALT

James Albright
University of California
Los Alamos National Laboratory, Los Alamos, NM 87545

Christopher Pearson
University of California
Los Alamos National Laboratory, Los Alamos, NM 87545

ABSTRACT

In November 1978, the Los Alamos National Laboratory installed a triaxial downhole geophone package at the Bryan Mound Strategic Petroleum Reserve, a salt dome near Freeport, Texas. Monitoring was for the purpose of detecting microseismic activity during the depressurization of one of the oil storage caverns. Seismic activity started soon after the start of depressurization, reached a peak 5 days later, and rapidly died off. Nineteen locatable microearthquakes with magnitudes between -1 and -2 were observed during and after depressurization. All but two of these events were located near the side of the oil storage cavern.

Because the shear wave spectra of these events were characterized by well-defined corner frequencies we were able to calculate the radius of the rupture surface, the seismic moment, and the stress drop from the source spectra. Estimates of the source radius vary from 15 to 100 m, stress drops range from 0.3 to 0.01 bar, and seismic moments range from [illegible] to [illegible] dyne/cm.

Important conclusions from this study are that comparatively small changes in the internal pressure of oil storage caverns may be enough to cause failure in the salt near the cavern walls and that downhole microseismic surveys can locate zones near large underground excavations that are undergoing rock failure.

INTRODUCTION

In recent years, large caverns leached in rock salt by fresh water have been widely used to store oil and liquid chemicals that are insoluble with water. In these systems, the liquid is stored as the upper part of a two-phase system floating on a pad of brine. The oil or chemicals can be removed by displacing an equivalent volume of brine or vice versa. Because the stored fluids have a lower density than water, the surface pressure of the fluid at the well head must be maintained at a high enough value to compensate for the difference in hydrostatic pressure between the stored fluids and brine (zero surface level brine pressure).

This paper describes a microseismic survey carried out by the Los Alamos National Laboratory over one such cavern (henceforth referred to as BM5) in an oil storage field operated by the Department of Energy's Office of Strategic Petroleum Reserve. Oil in this particular cavern was stored under a pressure of 1.1 MPa (160 psi) above zero surface level brine pressure. The oil pressure measured at the surface was reduced to zero surface level brine pressure during the work to be described.

At the time of depressurization, BM5 contained approximately 2 million cubic meters (5.3×10^{8} gal) of oil and the integrity of BM5 was in doubt because of a pinch-off of the drill string in the well originally used in mining the cavern, well 5. Oil side depressurization from 4.1 MPa (600 psi) to 3.0 MPa (440 psi) (approximately zero surface brine pressure) took place from 1900 hours on November 22 to 1315 hours on November 25, 1978.

The location of BM5 at the Bryan Mound site is shown in Figure 1.

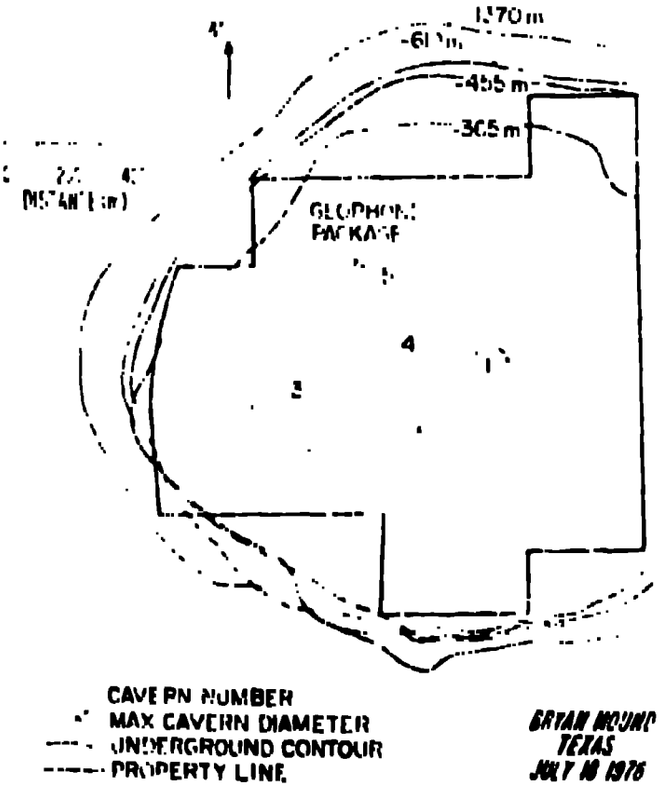

Figure 1 - Sketch map of the Bryan Mound National Strategic Petroleum Reserve (abstracted from a figure provided courtesy of Department of Energy Office of Strategic Petroleum Reserves.

This cavern is the northermost of five caverns at the site that were originally leached for brine. Mining of BM5 was accomplished through Well 5. The cavern is comprised of two cells; the lower cell is larger and has a maximum roof span of approximately 230 m (750 ft). Cavern pressures during mining probably never substantially deviated from that produced by a ground-level brine head. The brine-filled cavern was certified for oil storage by the Department of Energy (DOE) in 1978 by subjecting it to pressures 10% in excess of its expected nominal operating pressure. Oil storage was accomplished by brine displacement, which subjected the cavern to cyclic high stresses. During brine displacement, the brine head cycled over a 0.3 MPa (44 psi) pressure range while oil injection pressures cycled over a 1.7 MPa (250 psi) range constrained at the upper limit by a maximum operating pump pressure of 5.2 MPa (750 psi). The nominal storage pressure in BM5 is 4.1 MPa (600 psi) surface oil pressure.

Monitoring for microearthquakes started on November 11, continued until November 30, and encompassed the three-day period of cavern depressurization. The detection system -- a triaxial configuration of geophones designed for use in the DOE Hot Dry Rock Geothermal Energy Development Project [Dennis and others, 1976] -- was installed at a depth of 592 m (1942 ft) in well 5C, which (at that time) had a total depth of 595 m (1952 ft). The installation was in salt, approximately 274 m (900 ft) below the bottom of the cap rock sequence at Bryan Mound and within 76 m (250 ft) of the uppermost part of BM5.

INSTRUMENTATION

A schematic of the triaxial geophone package used at Bryan Mound is shown in Figure 2. The essential components of the system are the geophones, the power pack, the amplifiers, and the locking mechanism each designed for performance at high temperature. Twelve geophones in three sets of four are used. One set is comprised of geophones designed for response to vertical motions; the other two sets are designed for horizontal motion response. The three sets of geophones are referred to in succeeding sections of this paper as the vertical geophones, the horizontal-reference geophones, and, orthogonal to each of these, horizontal geophone set No. 2. The four geophones in each set are wired in parallel such that failure of up to three geophones can occur without complete loss of output. The combined amplification of each geophone-amplifier set is 2000. The geophones, Mark Product type L15A, have a natural frequency of 10 Hz and are designed to work at angles of up to 14° without noticeable degradation in response. The response of the geophones is essentially constant for frequencies above 100 Hz (21.1 V/m/s). The three differential amplifiers were each powered by a pack of eight 12-volt batteries. The lifetime of the battery pack is 2000 mA-h, which assures 48 days of continuous operation with the amplifiers in saturation.

The downhole package is dumbbell shaped with the geophones housed in the upper bell. When the package is in position downhole, a motor-driven arm is extended so that the package contacts the walls of the borehole at three points. The geophone package once installed remained in place for 14 days. The orientation of the geophone package was neither controlled nor known on installation but later determined by

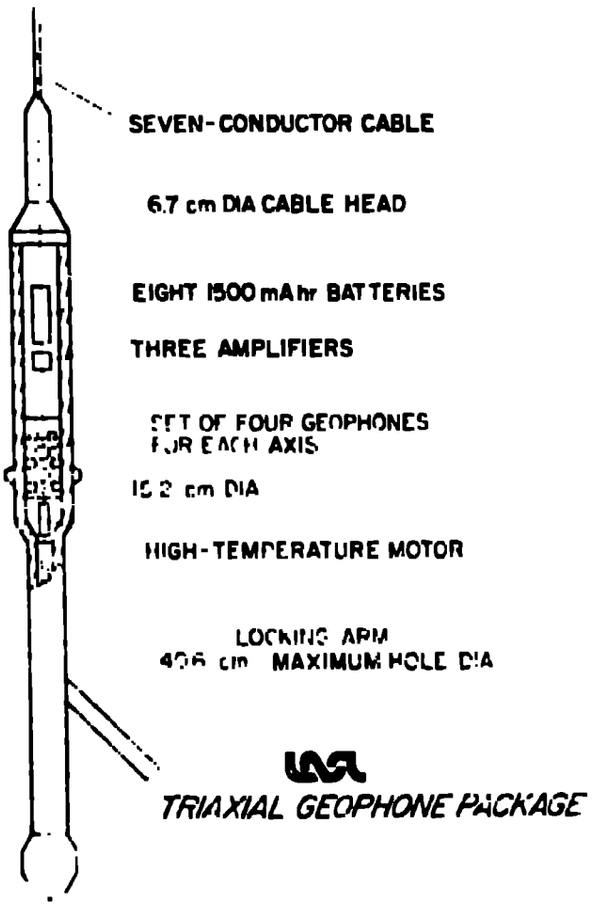

Figure 2 - Schematic of the Los Alamos triaxial geophone package used to monitor the microseismic activity associated with the depressurization of EM5.

measuring the azimuths to explosives detonated at the surface. An additional, single, vertical geophone, identical to the vertical geophones used in the downhole package, was mounted on the blowout preventer attached to the surface casing at the wellhead at 5C. Output from this geophone was amplified by a factor of 50. This unit, served a particularly useful purpose in that records from this geophone could be compared to those from downhole to identify signals that clearly originated at the surface but were also detected by the downhole package.

Microseismic events which have clear P- and S-arrivals can be located using a single 3-component downhole geophone package. The azimuth to an event can be determined using the relative signal amplitudes of the P-wave first motion record along each axis. The distance to the signal can be calculated from the delay time between S-wave and P-wave arrivals, if the propagation velocity of the respective phases is

known. Clearly there is a 180° ambiguity in the location of an event if only one detection station is used, since the sense of the first motion at the source is not known. However, because of the location of the geophone package during this survey, only one of the two possible locations for each event was considered likely.

MICROSEISMICITY NEAR CAVERN 5

A histogram giving a count of the microearthquakes occurring in 2-h intervals throughout the 19-day monitoring period is given in Figure 3. Also shown is an idealized plot of RM5 pressure throughout the same period. Noise arising from surface construction activities precluded identification of microseismic signals from daytime records. Below the histogram we have plotted a solid bar indicating times when low-noise records were obtained.

Thirty-four events were detected, the first soon after the start of cavern depressurization. Of these 34, 19 events were of sufficient quality to be processed for further information. Except for two microearthquakes, all locatable microseismic activity occurred in very close proximity to the RM5 cavern walls. The locations of the microearthquake epicenters are shown in Figure 4. The locations of the microearthquakes originating near RM5, shown in Figure 4, are plotted in Figure 5 as foci projected onto the vertical EW plane intersecting RM5 and containing Well 5. The signal identification numbers used in later analysis are also given.

Without exception, the signals generated by microearthquakes occurring near RM5 show a compressive signal arrival on records of the vertical geophone unit, followed in time by a second arrival prominent on the horizontal geophone records. Examples of these signals are given in Figure 6. The first arrival was taken as that of the compressional (P) wave and the second as that of the shear (S) wave. S-P delays for the microearthquakes detected range from 5 to 20 ms. Mapped epicenters near Cavern 5 are anticipated to be accurate to ±5 m (±15 ft) in depth and to ±15 m (±50 ft) in distance.

It is not surprising that the microearthquakes that were detected near RM5 occurred at high inclinations to the geophone package. Figure 5 shows the regions of nonlocatable microearthquakes, indicating that events could have occurred in large volumes of rock adjacent to RM5 without being detected, or, if detected, their signals would not contain the requisite information to allow event location. This is because direct transmission paths between microearthquake foci in this region and the geophone package would have to pass through the cavern. As a consequence, the shear-wave portion of the microseismic signals would be lost and the compressional wave portion attenuated and reflected by the cavern/salt interface, making location of the event impossible. Two microseismic events were detected in the 640- to 670-m (2101- to 2198-ft) interval near the western corner of the ceiling of the upper cavern cell. Several events, closely grouped together, were detected in the depth intervals of 762 m (2500 ft) to 792 m (2600 ft), the lower part of the upper cell, and from 832 m (2729 ft) to 869 m, (2947 ft) near the ceiling of the lower cavern cell. A few were

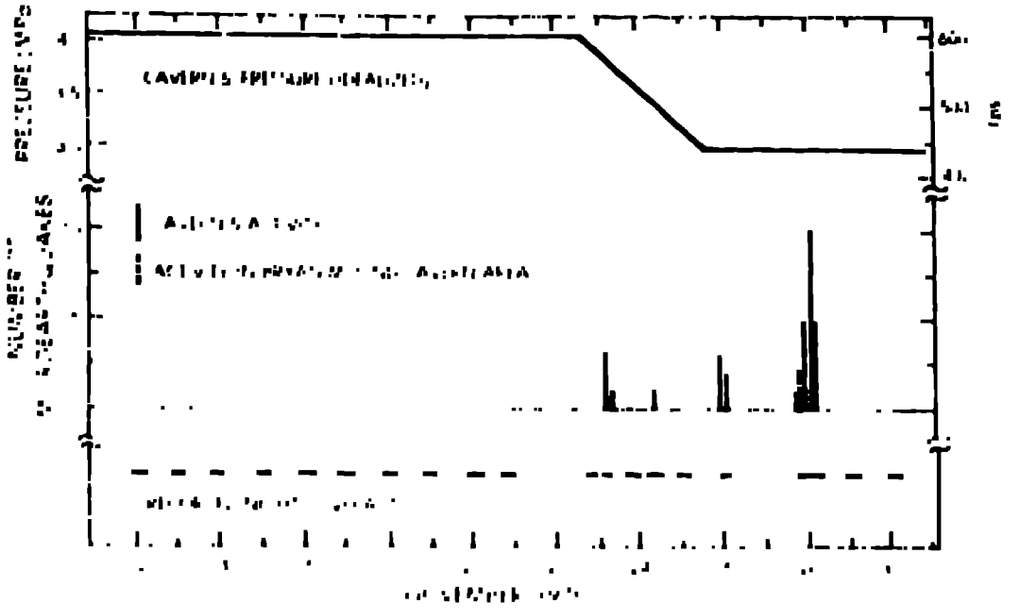

Figure 3 - Recording coverage, microearthquake count, and idealized pressure history during the depressurization of BM5.

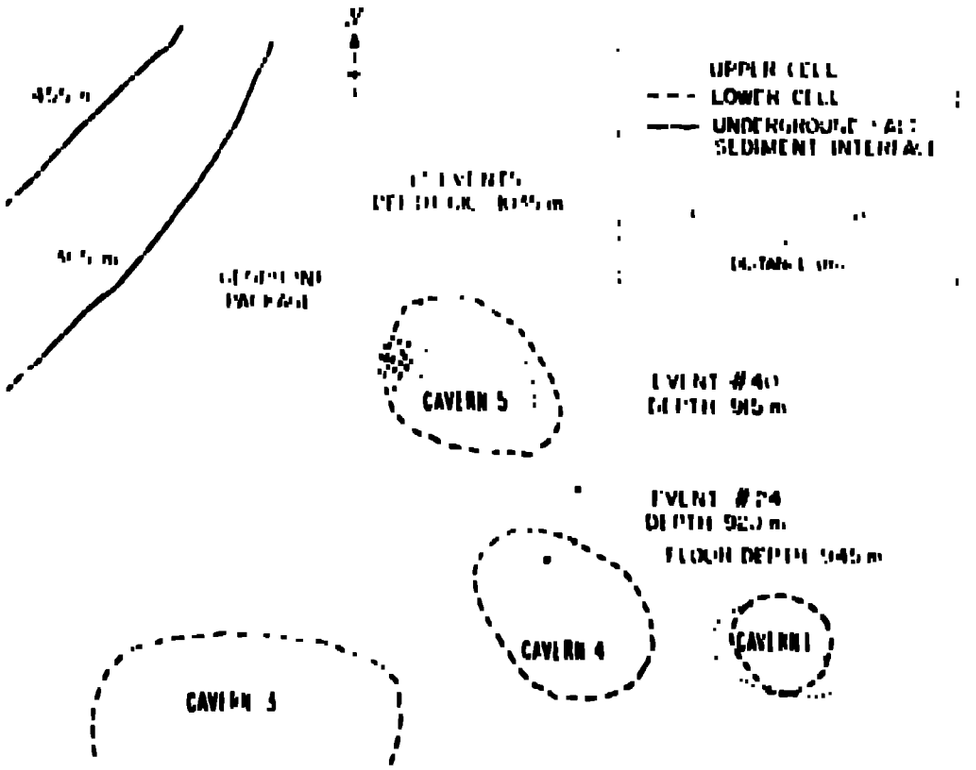

Figure 4 - Epicentral locations of the microearthquakes detected at Bryan Mound.

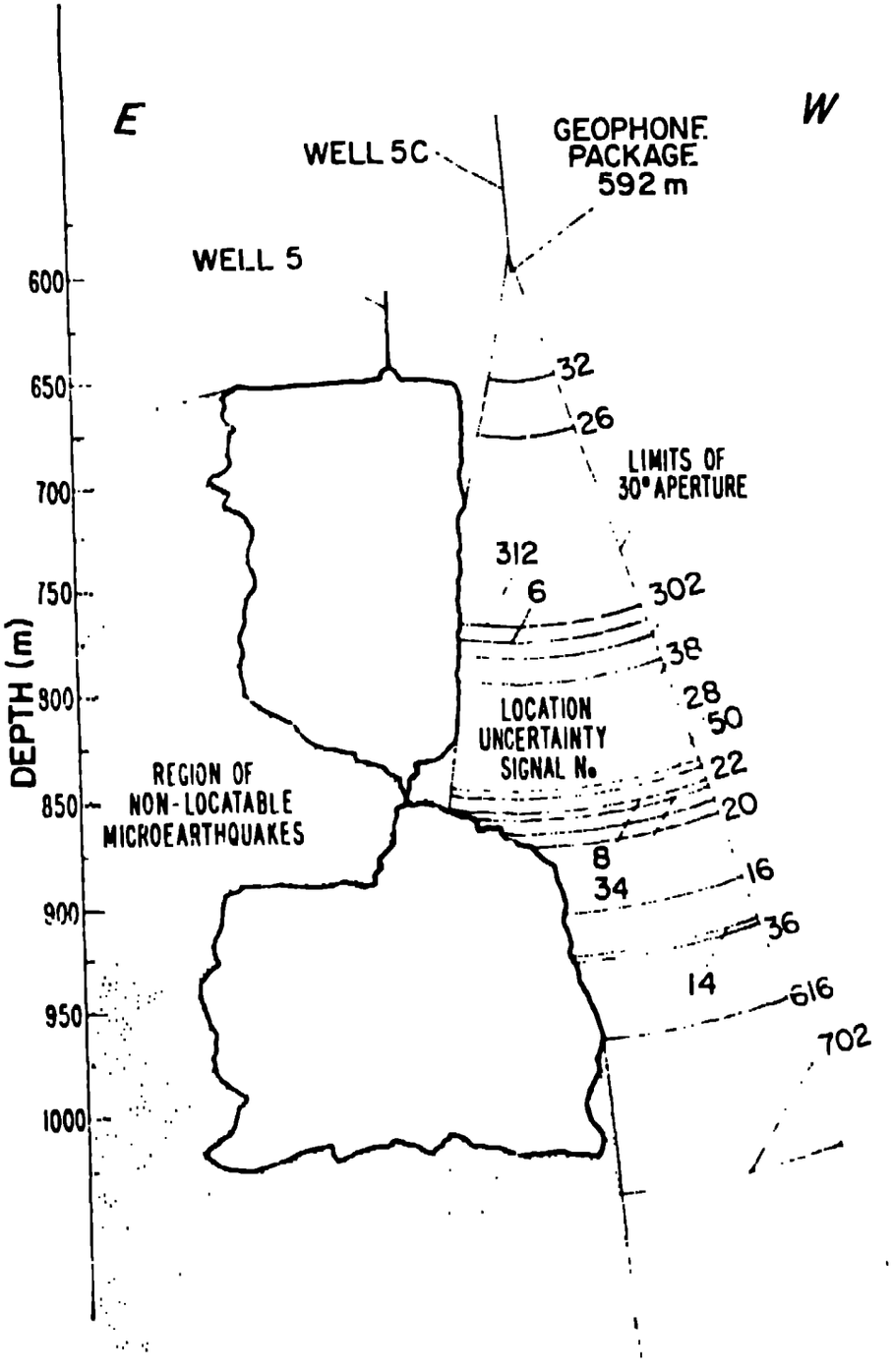

Figure 5 - Projection of microearthquake foci onto east-west cross section of BM5 that contains Well 5.

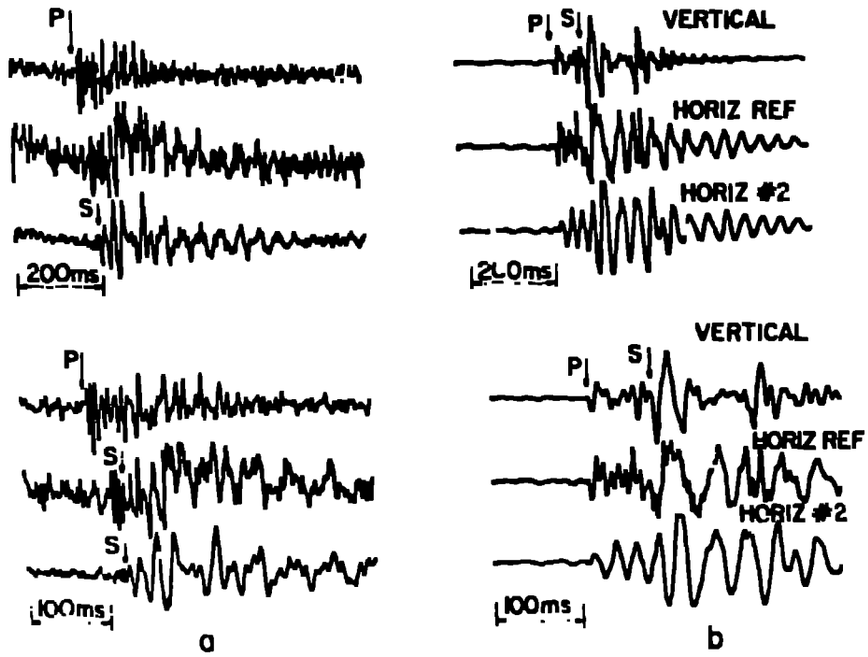

Figure 6 - Triaxial geophone records of events 8, 24, 26, and 34; (a), (b), (c), and (d) respectively.

detected in the 884-m (2900-ft) to 1006-m (3300-ft) interval at depths corresponding to those of the lower cavern cell.

SOURCE PARAMETER ANALYSES

Using a model proposed by Brune [1970], it is possible to estimate microearthquake source properties--specifically seismic moments, source dimensions, and stress drops--from spectral data. Brune's model predicts that the amplitude spectrum of the shear-wave displacement data should be characterized by two trends; a low-frequency, constant-spectral-amplitude trend, and a high-frequency trend in which the spectral amplitude decreases at $1/f^2$, where f is the frequency. Using the average value of the constant, low-frequency trend (Ω_0), and the frequency of the intersection of the two trends (the corner frequency f_c), it is possible to estimate source parameters. The relevant formulae for the source dimension (r), the seismic moment (M_0) and the stress drop ($\Delta\sigma$) [Tucker and Brune, 1973] are

$$r = \frac{2.34}{2\pi} \beta \frac{1}{f_c} \qquad (1)$$

$$M_0 = \frac{4\pi\rho R\beta^3 \Omega_0}{KR_{\theta\phi}} \qquad (2)$$

$$\Delta\sigma = \frac{7}{16}\frac{M_o}{r^3} \qquad (3)$$

where, for our purposes, β and ρ are the shear-wave velocity and density of the salt surrounding BM5, respectively, R is the distance to the microearthquake focus, $R_{\theta\phi}$ is a correction factor for the detector's position within the shear-wave radiation pattern about the microearthquake focus, and K is a correction factor for amplification from free surface reflection. The average salt density (1900 kg/m^3 or 1.9 g/cm^3) near BM5 was estimated from a Schlumberger density log taken in Well 5C. A root-mean-square value of 0.4 was used for $R_{\theta\phi}$ since the radiation pattern of microearthquakes cannot be deduced from the single measurement made at the geophone package. As the geophone package was positioned at depth within the dome and not near ground level, K was assumed to be equal to 1. No attempt was made to take into account the effect of seismic radiation reflected at the walls of the cavern although this may result in a correction similar to K.

Seismic source parameters were calculated from amplitude displacement spectra for all of the located earthquakes except for those with identification numbers 302, 312, and 6. Figure 7 gives examples of the displacement spectral density plots. In all cases, except for events 24 and 40, the spectrum was derived from signals detected on whichever of the two horizontal geophones had the stronger S-wave arrival. This was appropriate because all but two of the located events (i.e., events 24 and 40) were, to within measurement error, directly beneath the geophone package. Because S-wave particle motion is polarized in a plane perpendicular to the ray path and P-wave motion is always polarized in the direction of signal propagation, the use of the trace from the horizontal geophones maximized the S-wave and minimized the P-wave particle motion contribution in the computed spectra.

The calculated source dimensions (r) of the microearthquakes studied ranged from 14 to 83 m. Of the events in proximity to BM5, those with the highest calculated stress drops originated in the region between the upper and lower cells of BM5 and near the bottom of the lower cell.

We estimated the local magnitudes using an empirical relationship between local magnitude (M) and seismic moment developed by Spottiswoode and McGarr for microearthquakes associated with rock failure in a deep gold mine. We chose their formula,

$$M = 0.714\ (\log M_o - 17.0)$$

because it was developed for microearthquakes with magnitudes ranging between -1 and 2 (near our expected magnitude range) and because (like the Bryan Mound microearthquakes) the events were caused by excavating large underground cavities. Clearly equation (1) can give at best only a rough estimate of the local magnitude. Table I is a summary of information deduced from spectral studies of Bryan Mound microseismic events.

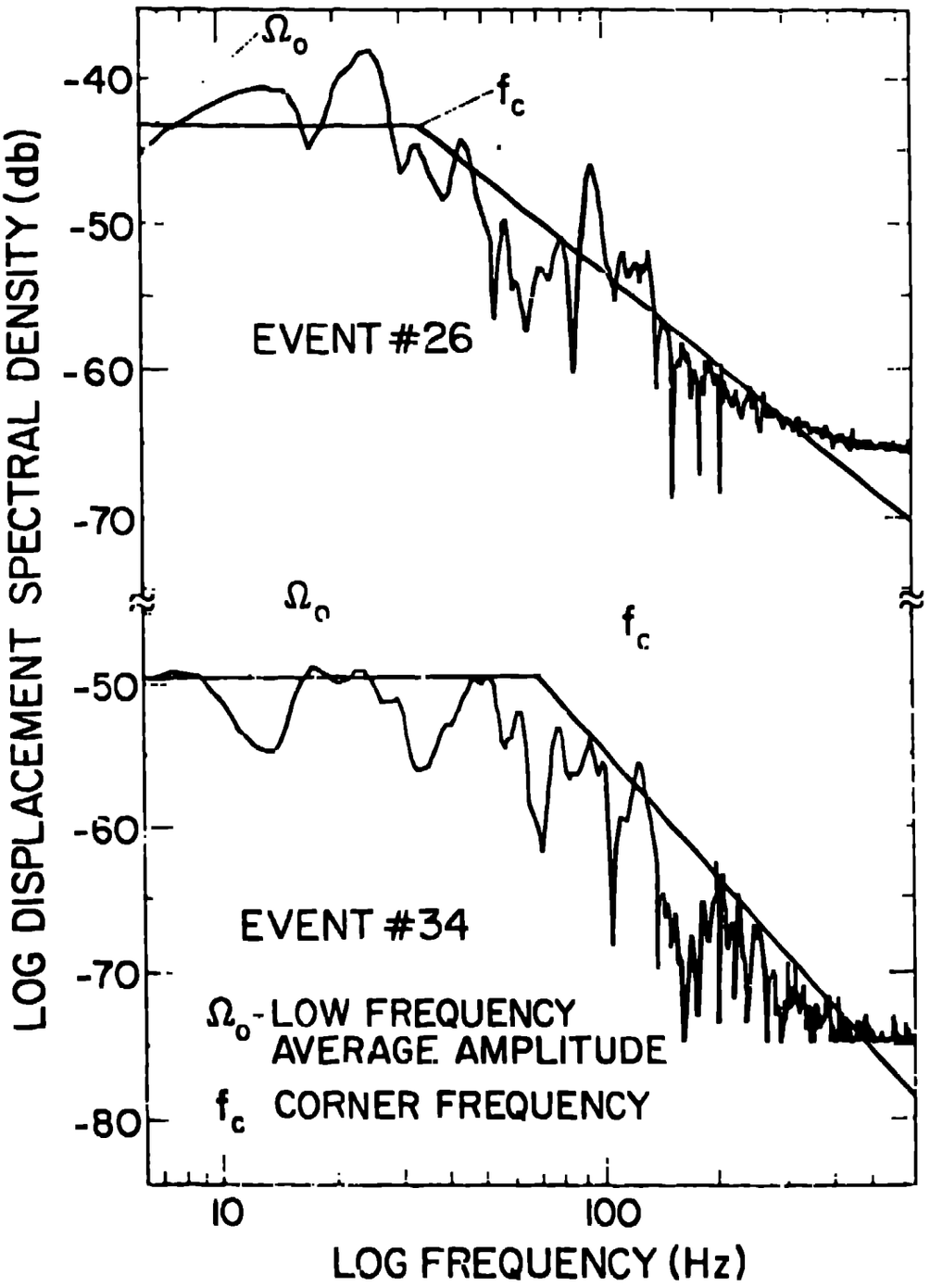

Figure 7 - Displacement spectral density plots used in determining source parameters for (a) event 26 and (b) event 34.

TABLE I

SUMMARY OF INFORMATION REDUCED FROM SPECTRAL STUDIES ON BRYAN MOUND MICROSEISMIC EVENTS

Event Number	Corner Frequency (Hz)	r (m)	M_o (10^{**} Joule)	10^{**} $\Delta\sigma$ MPa	Local Magnitude
32	52	19	3	7	-1.8
26	34	29	15	3	-1.3
[illegible]	34	29	6	2	-1.6
28	[illegible]	17	25	23	-1.1
50	60	[illegible]	3	2	-1.9
[illegible]	61	16	2	4	-1.8
46	[illegible]	[illegible]	6	3	1.6
27	60	17	8	7	-1.5
[illegible]	[illegible]	16	5	7	-1.6
17	[illegible]	41	6	1	-1.5
14	17	[illegible]	14	1	-1.3
[illegible]	[illegible]	19	6	5	-1.6
[illegible]	[illegible]	[illegible]	19	8	-1.4
24	33	[illegible]	21	6	-1.2
7	[illegible]	35	15	22	-1.3
21	[illegible]	[illegible]	7	22	-1.8

Savage and Wood [1971] demonstrate that the mean shear stress acting on a fault $\bar{\sigma}$ and the stress drop during an earthquake are related by $\eta = 1/2\ \frac{\Delta\sigma}{\bar{\sigma}}$ where η is the seismic efficiency or the ratio of the seismic energy released during an event to the total strain energy released. Estimates of the seismic efficiency range from a few percent to a few tenths of a percent. Even if we assume that the lowest reported figures are correct, equation (2) implies that the mean shear stress acting on the fault planes in Bryan Mound was on the order of a few bars. Since this is much less than the shear strength of rock salt, these events are probably associated with renewed slippage on pre-existing fractures or planes of weakened competent rock salt.

CONCLUSION

Slight structural adjustments occurred during depressurization of Cavern 6 as evidenced by the detected microearthquake activity. These changes were likely the result of slippage on pre-existing fractures rather than from the creation of new fractures. The slippage was

reactivated by changes in cavern pressure. Assuming that the calculated microearthquake source dimensions are crudely correct, the existence of fractures extending tens of meters away from the cavern is implied. Hydraulic communication of these fractures with the cavern is possible. Further, stress interaction between caverns 4 and 5 is suggested by events 24 and 40.

The results of this study suggest that downhole microseismic surveys can provide detailed information on the location and extent of rock failures associated with oil storage caverns located in salt. Such downhole techniques may well be applied to the stability evaluation of other large structures such as gas storage caverns, pump storage facilities, tunnels, and mines.

ACKNOWLEDGMENTS

The authors thank the following individuals who functioned in support of the planning and execution of the field operations at Bryan Mound: William Root, SPR Bryan Mound Site Manager; Harro Lorenzen and Ted Nielson of PB-KBB Inc.; Charles Bellam, Bryan Mound Resident Engineer; Thomas Weaver, John Stewart and Rosco Butler, Los Alamos National Laboratory. We particularly acknowledge the contribution of Paul Smith, Robert Bridwell, and C. A. Anderson for the finite element calculations that facilitated the interpretation of Bryan Mound data.

REFERENCES

Brune, J. N., [1970], "Tectonic Stresses And The Spectra of Seismic Shear Waves from Earthquakes," J. of Geophys. Res., vol. 75,

Dennis, B. R., Hill, J. L., Shephard, L. E., and Todd, R. F., [1976], "Development of High Temperature Acoustic Instrumentation for Characterization of Hydraulic Fractures in Dry Hot Rock," 22nd International Instrumentation Symposium, San Diego, California.

Hanks, T. C. and Wyss, M. P., [1971], "The Relation Between Apparent Stress and Stress Drop," Bull. of the Seismol. Soc. of Amer. vol. 61, 1367-1378.

Hartzell, S. H. and Brune, J. N., [1974], "Source Parameters of Aftershocks in a Deep Level Gold Mine," Bull. of the Seismol. Soc. of Amer. vol. 64, 1-11.

Luetgert, R. F. and Brune, J. N., [1974], "Seismograms, P-Wave Spectra and Source Parameters for Aftershocks of the San Fernando Earthquake," San Fernando Earthquake of February 9, 1971, vol. 1, Neil A. Bonilla, Mary V. Duffield and John R. Hamish, Eds., U.S. Dept. of Commerce, [illegible].